The C-terminal helical bundle of the tetrameric prokaryotic sodium channel accelerates the inactivation rate

Katsumasa Irie[1, 2], Takushi Shimomura[1], and Yoshinori Fujiyoshi[1, 2].

[1]Department of Biophysics, Graduate School of Science, Kyoto University, Oiwake, Kitashirakawa, Sakyo-ku, Kyoto, Japan, 606-8502. [2]Japan Biological Informatics Consortium, Oiwake, Kitashirakawa, Sakyo-ku, Kyoto, Japan 606-8502.

Supplementary Information

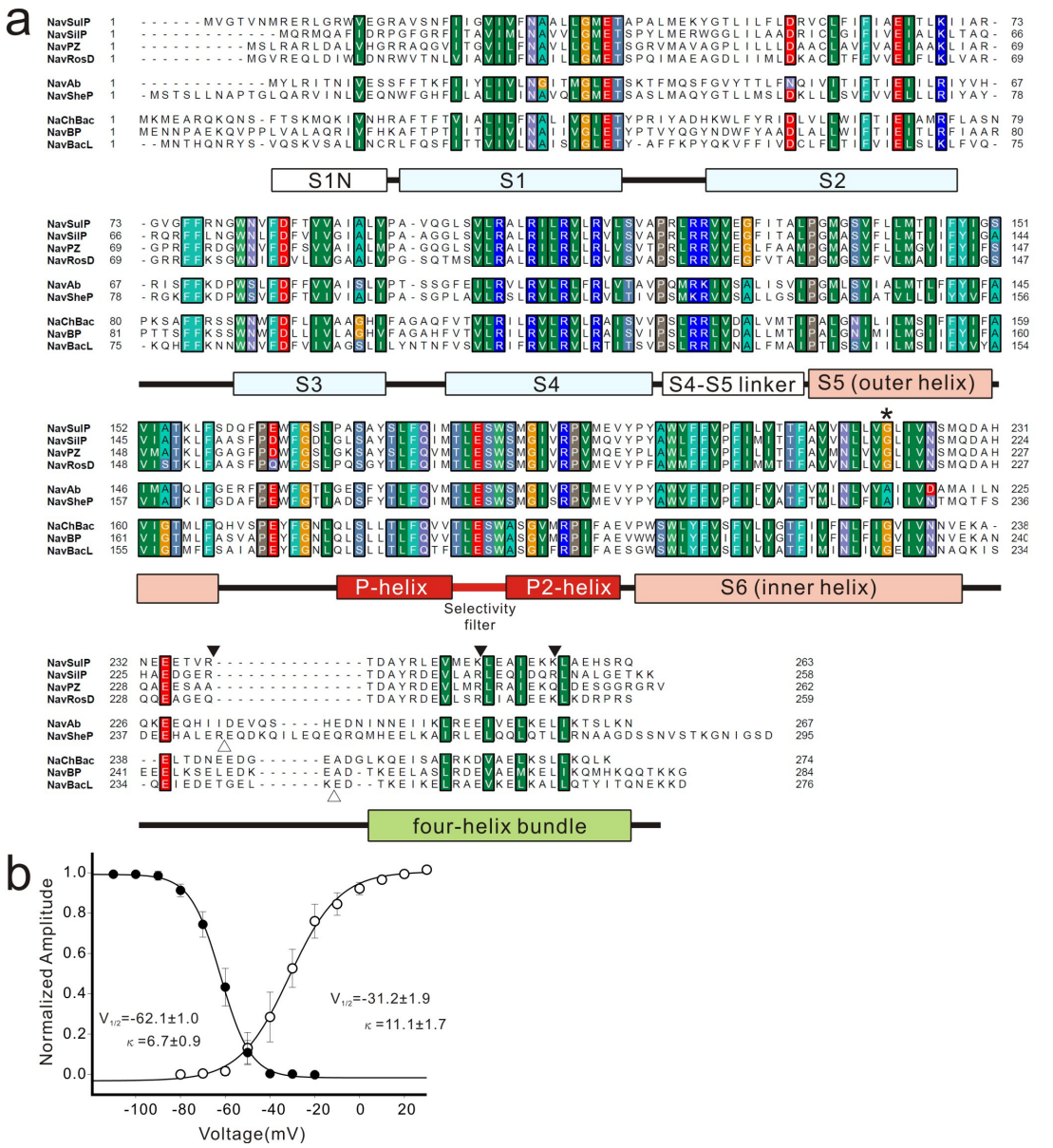

Supplementary Figure S1. Primary sequence and voltage dependency of NavSulP

(**a**) Alignment of the amino acid sequences of NavBacs. The diagram of the secondary structure is referenced to the structure of NavAb and NaK-NavSulP chimera channel. Cylinders and solid lines indicate α-helix and loop structures, respectively. Filled triangle indicates the C-terminal deletion position of NavSulP. Open triangle indicates the deletion position of NavBacL and NavSheP. Asterisk indicates the position of the conserved glycine of the inner helix. (**b**) Voltage-dependent activation and inactivation of NavSulP. The deactivation tail currents of NavSulP are indicated by the open circle (*n*=9). After prepulses of varying depolarisation, tail currents were measured at -120 mV. The steady-state inactivation currents of NavSulP are indicated by the filled circle (*n*=6). After a 2-s prepulse, the channels were inactivated to a steady-state level and reactivated by a second depolarisation pulse (+20 mV). All values are presented as mean ± standard error.

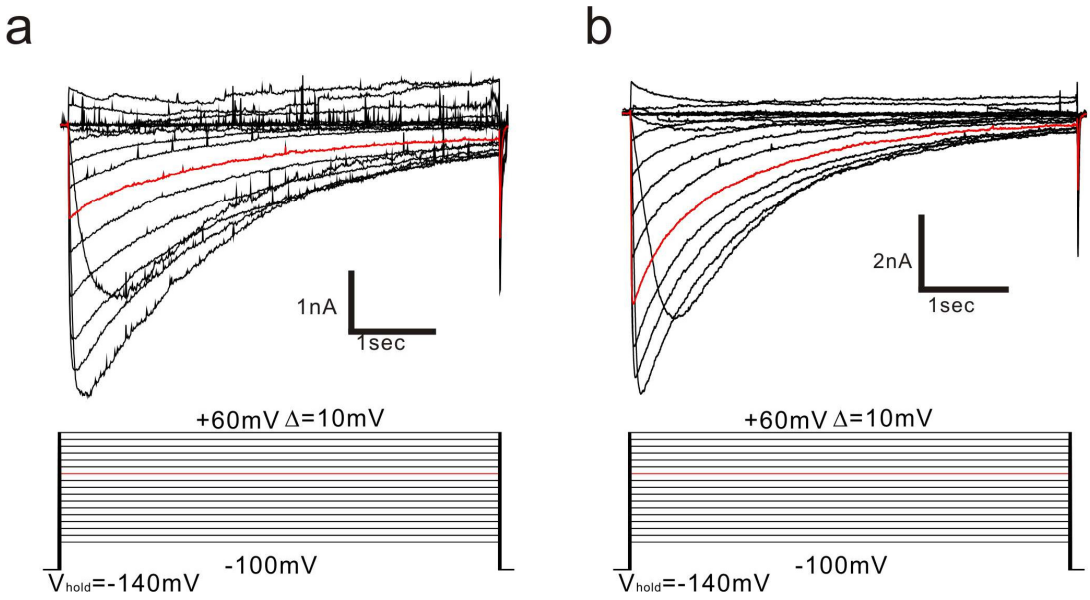

Supplementary Figure S2. Representative trace of the C-terminal deletion mutation of NavSulP

(**a**) and (**b**) Representative traces of the current of NavSulPΔC250 and ΔC257 resulting from the voltage protocol shown below, respectively. The current traces and voltage protocols in red were obtained at 0 mV membrane potential.

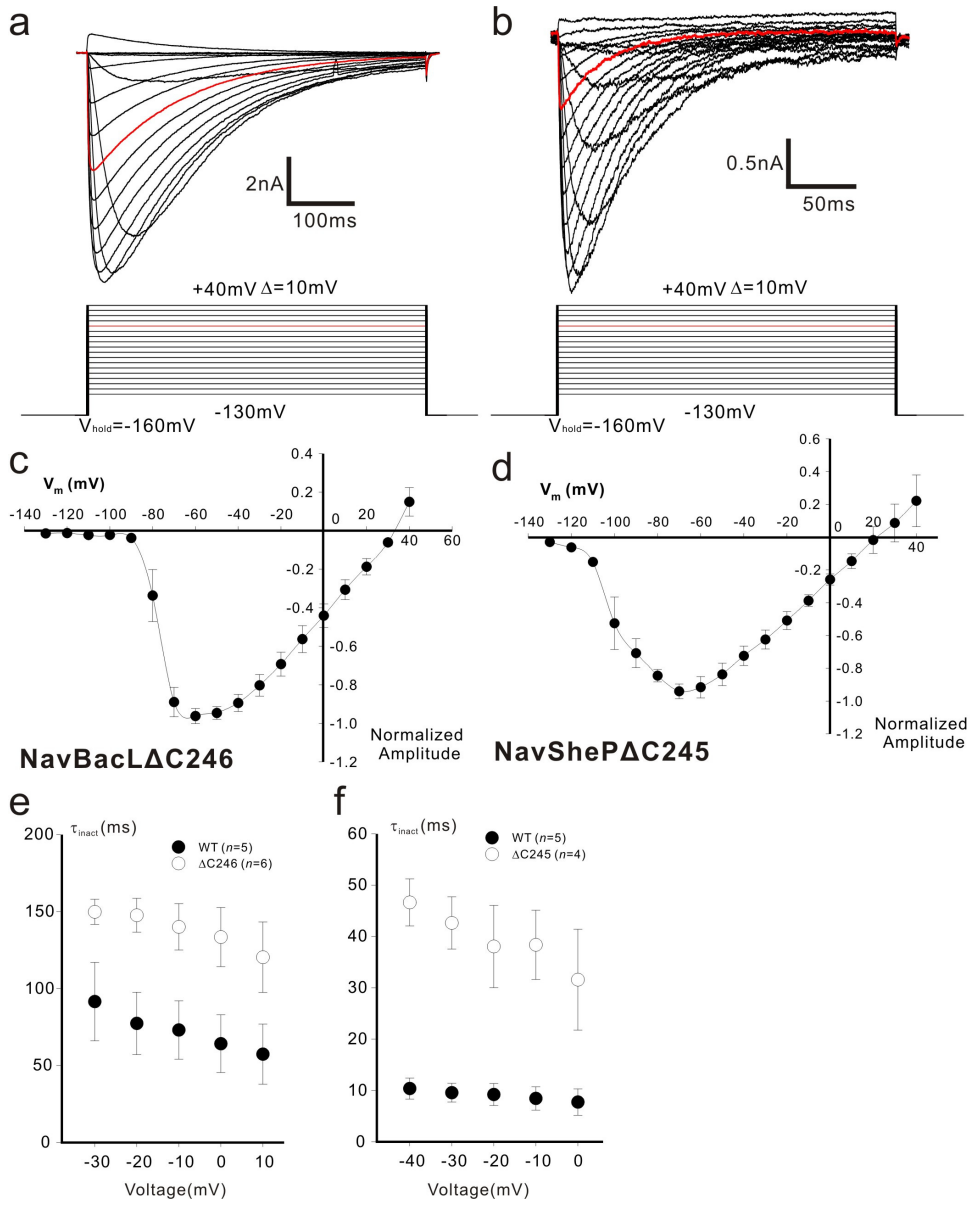

Supplementary Figure S3. The channel activity of the C-terminal deletion mutant of NavBacL and NavSheP

(**a**) and (**b**) Representative traces of the current of NavBacLΔC246 and NavShePΔC245 resulting from the voltage protocol shown below, respectively. The current traces and voltage protocols in red were obtained at 0 mV membrane potential. (**c**) and (**d**) Mean peak current-voltage relation of NavBacLΔC246 (*n*=6) and NavShePΔC245 (*n*=4) normalised by the peak current, respectively. (**e**) and (**f**) The inactivation time constants (τ_{inact}) of wild-type and C-terminal deletion channels of NavBacL and NavSheP measured from the current traces elicited by step pulses from holding potential at -160 mV. The value of τ_{inact} was defined as the time from the peak current to 1/e of the peak current. All values are presented as mean ± standard error.

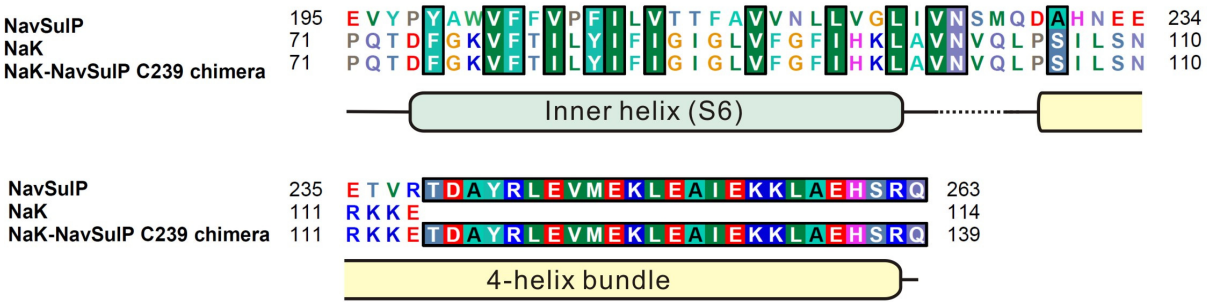

Supplementary Figure S4.

Alignment of the amino acid sequences of inner helix of NavSulP, NaK channel, and NaK-NavSulP C239 chimera channel together with the diagram of the secondary structure of the chimera channel. Cylinder and solid line indicate the α-helix and loop structure, respectively. Dashed line indicates the residues that were not observed in chain B, but were observed in chain A.

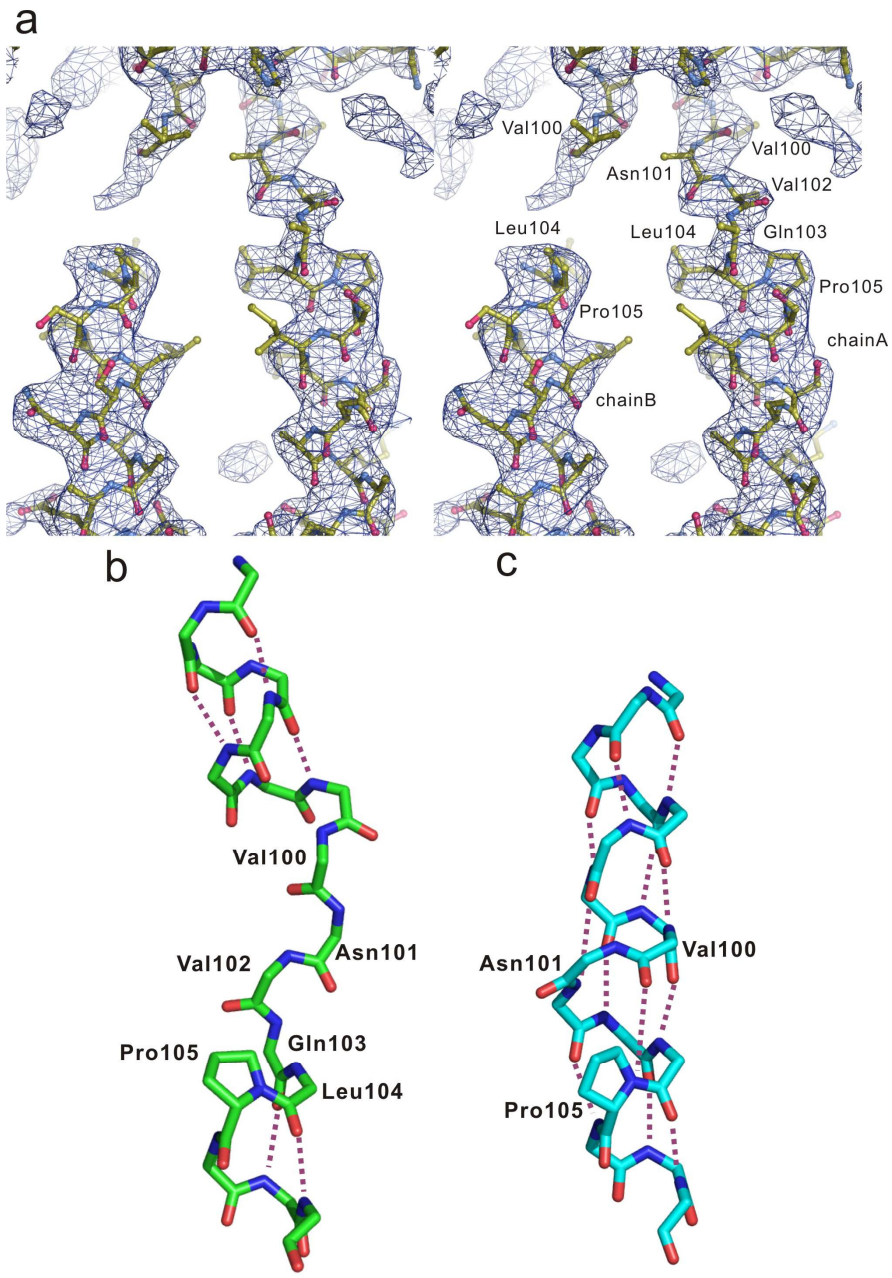

Supplementary Figure S5.

(**a**) Stereo view of 2Fo-Fc electron density map of NaK-NavSulP C239 chimera channel contoured at 1.0 σ. The electron density of the residues from Asn101 to Gln103 of chain B was not observed clearly. The electron density of the side-chain of those residues of chain A was also not observed. (**b**) and (**c**) Comparison of the hydrogen bonding network of Pro105 between the NaK-NavSulP chimera channel (b) and NaK channel (c). The backbone of the NaK-NavSulP chimera channel (green) and NaK channel (cyan) from Phe92 to Leu108 is indicated in b and c, respectively.

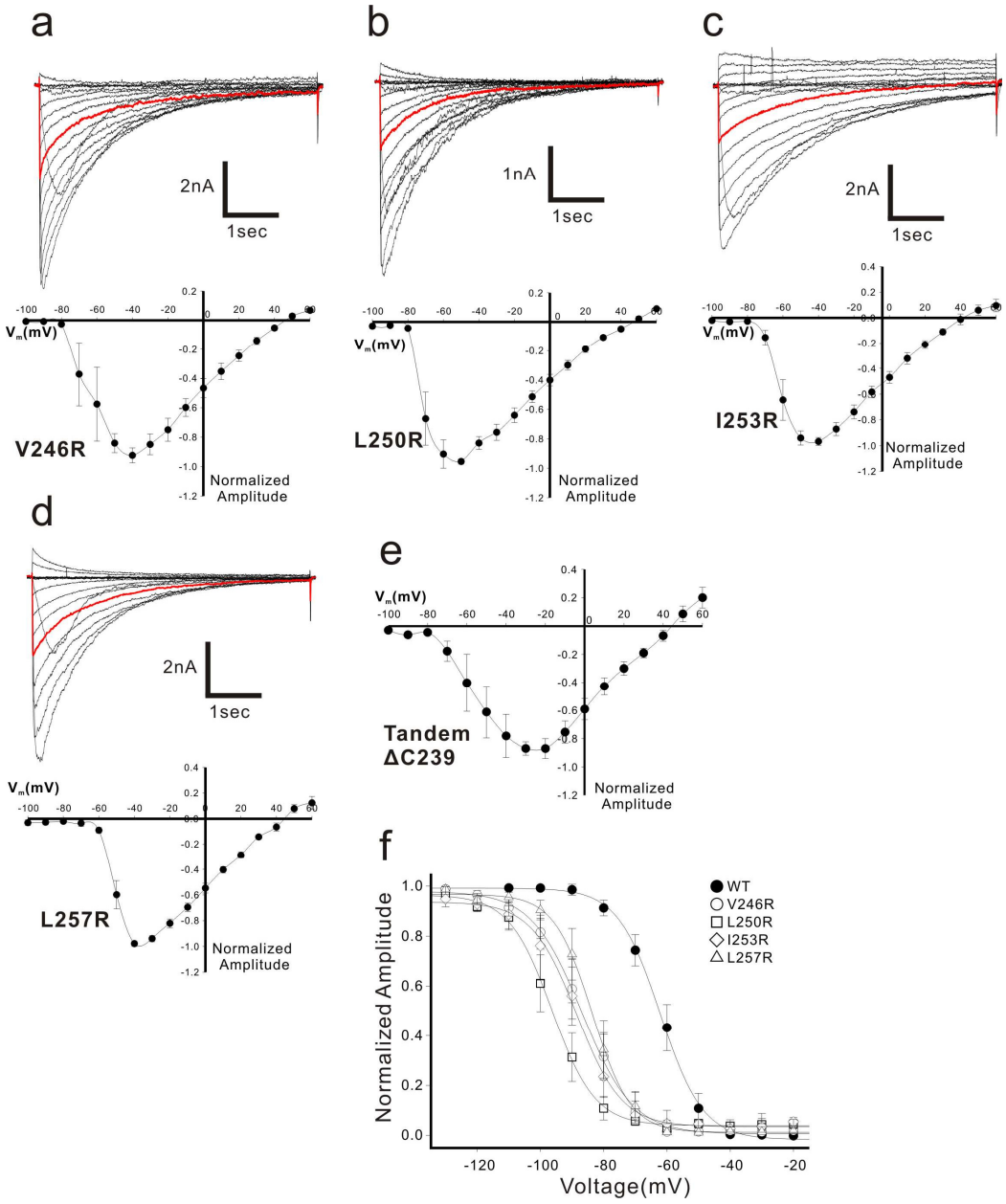

Supplementary Figure S6.

(**a**)-(**d**) Representative traces of the current and the mean peak current-voltage relation of NavSulP V246R (*n*=4), L250R (*n*=4), I253R (*n*=4), and L257R (*n*=5), respectively. All currents resulted from same voltage protocol as that of the C-terminal deletion mutants. The current traces in red were obtained at 0 mV membrane potential. (**e**) The mean peak current-voltage relation of NavSulP tandemΔC239 (*n*=5). (**f**) The steady-state inactivation curves for V246R (*n*=6), L250R (*n*=6), I253R (*n*=6), and L257R (*n*=5) mutants, and wild-type NavSulP (*n*=6). After a 15-s prepulse, the mutant channels were inactivated to a steady-state level and reactivated by a second depolarisation pulse (+20 mV). All values are presented as mean ±standard error.

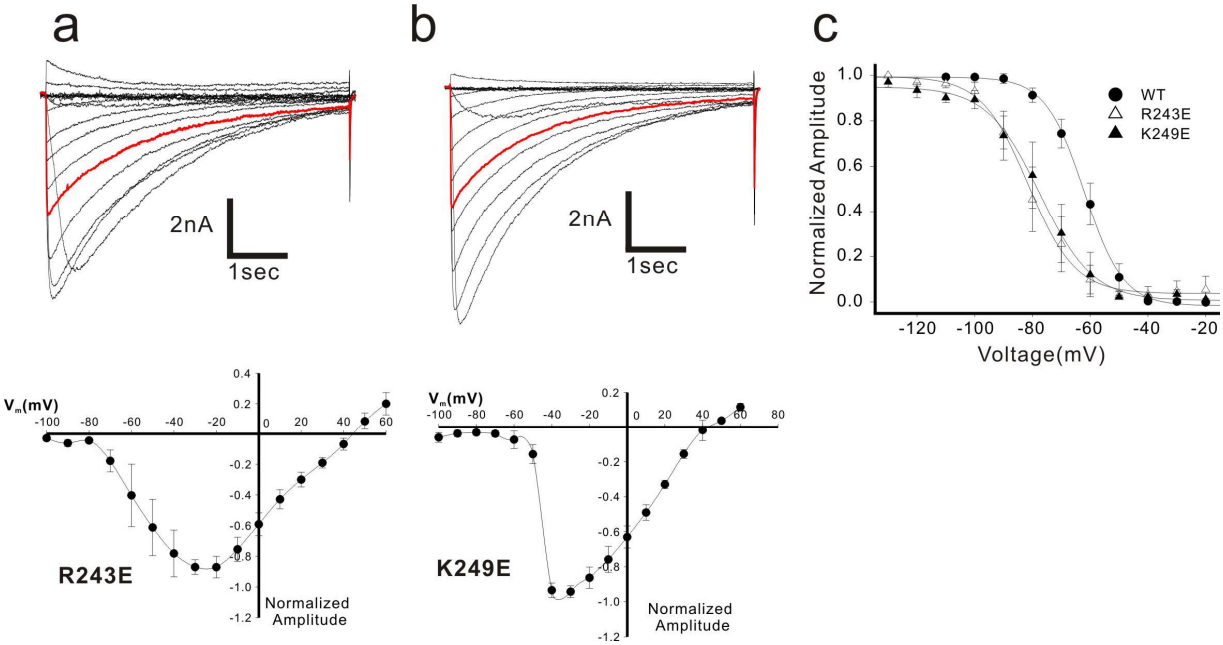

Supplementary Figure S7.

(**a**) and (**b**) Representative traces of the current and mean peak current-voltage relation of NavSulP R243E (*n*=4), and K249E (*n*=5), respectively. All currents resulted from the same voltage protocol used with the C-terminal deletion mutants. The current traces in red were obtained at 0 mV membrane potential. (**c**) The steady-state inactivation curves for R243E (*n*=5) and K249E (*n*=6) mutants and wild-type NavSulP (*n*=6). After a 15-s prepulse, the mutant channels were inactivated to a steady-state level and reactivated by a second depolarisation pulse (+20 mV). All values are presented as mean ± standard error.

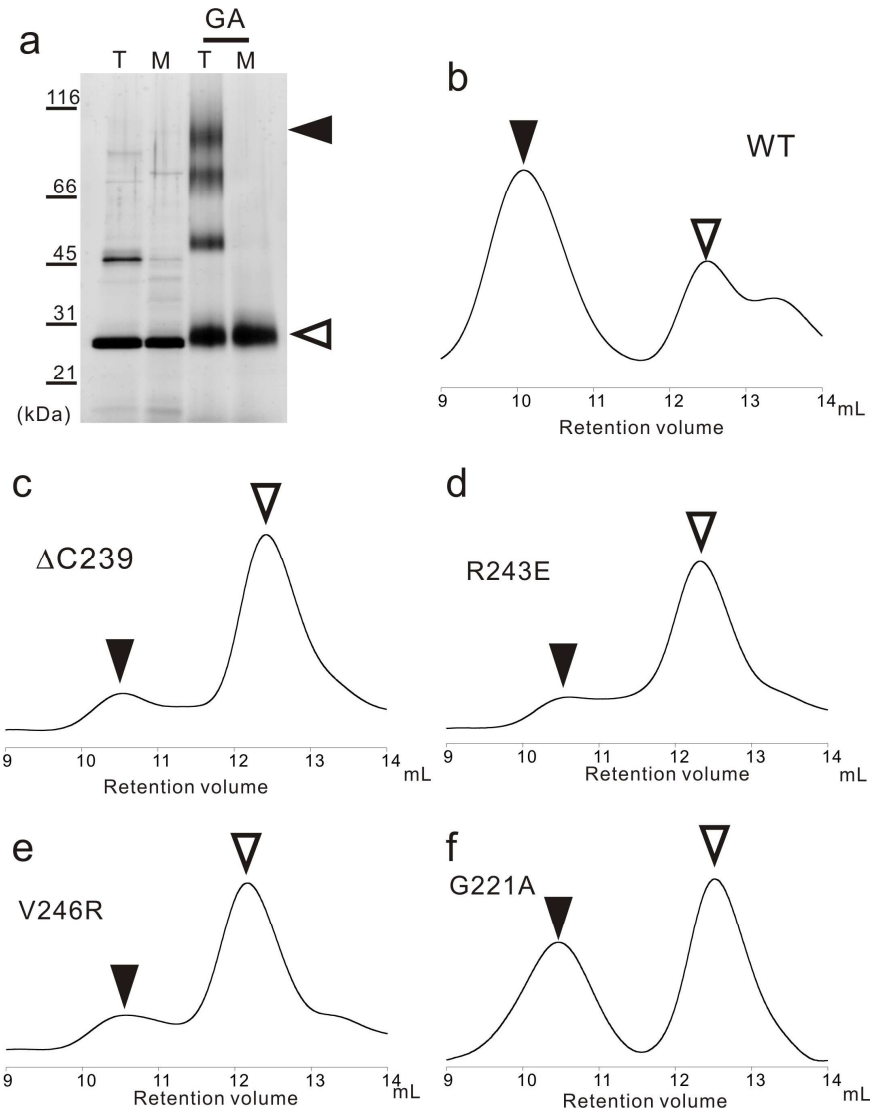

Supplementary Figure S8.

(**a**) The cross-linking reaction of purified wild-type NavSulP protein with glutaraldehyde. Purified proteins were resolved on sodium dodecyl sulphate-polyacrylamide gel electrophoresis analysis after cross-linking treatment with 1.0 mM glutaraldehyde. T and M indicate the tetramer and monomer fractions of NavSulP wild-type protein (b) in size-exclusion chromatography, respectively. GA indicates the glutaraldehyde-treated fractions. Tetramers cross-linked by glutaraldehyde are indicated by the filled arrowheads and monomers are indicated by the open arrowheads. In the non-cross-linking condition, almost all of the NavSulP protein migrated as monomer molecules in sodium dodecyl sulphate-polyacrylamide gel electrophoresis. (**b**)**-** (**f**) Size-exclusion chromatography profiles of NavSulP wild-type and mutants. The tetramer fraction is indicated by the filled arrowheads and the monomer fraction is indicated by the open arrowheads.

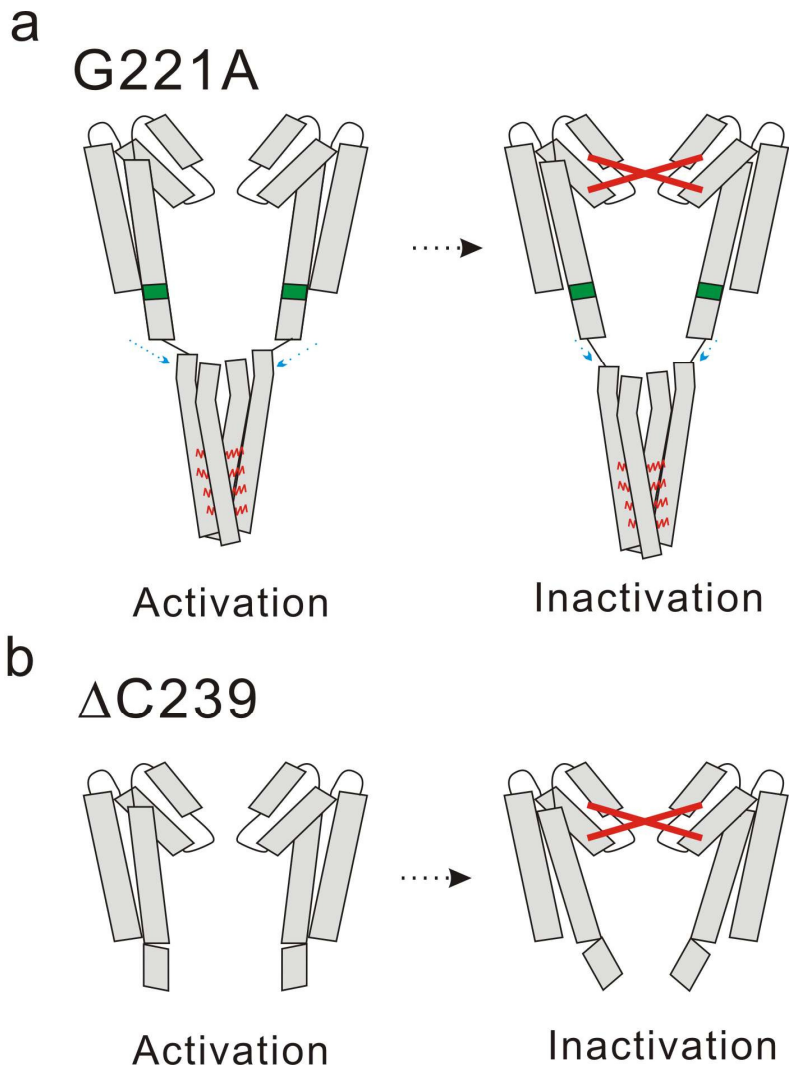

Supplementary Figure S9.

Hypothetical model of the inactivation of NavSulP G221A and ΔC239**.**

The front and rear subunits of the transmembrane part were removed for clarity. The red lines in the 4HB indicate the interaction of the hydrophobic core. The dashed black arrows indicate the slow transition from the open state to the inactivated state. (**a**) Hypothetical model of the inactivation of NavSulP G221A. The green part of the inner helix indicates the inner helix stabilised by the G221A mutation. The dashed blue arrows of NavSulP G221A indicate the weak pulling effect of the 4HB formation to the inner helix stabilised by the G221A mutation. The 4HB formation would require more time to promote the conformational change of the rigid inner helix of NavSulP G221A than that of wild-type NavSulP. (**b**) Hypothetical model of the inactivation of NavSulP ΔC239. The hinge of the inner helix indicates the position of Gly221. The inner helix of C-terminal deletion NavSulP would be free from the counter force of the 4HB formation, and spontaneously enter into the inactivated state with a slower rate.

Supplementary Table S1

Summary of the values of $V_{1/2}$ for inactivation.

	$V_{1/2}$ for inactivation (mV)											
NavSulP WT	-62.1	±	1.0	(κ=	6.7	±	0.9	)	(*n*=	6	)
ΔC239	-85.4	±	0.8	(κ=	7.1	±	0.7	)	(*n*=	6	)
ΔC250	-89.2	±	0.3	(κ=	6.9	±	0.3	)	(*n*=	4	)
ΔC257	-76.0	±	0.7	(κ=	9.8	±	0.7	)	(*n*=	6	)
Tandem WT	-72.0	±	1.0	(κ=	11.4	±	0.9	)	(*n*=	5	)
TandemΔC239	-86.6	±	0.4	(κ=	7.4	±	0.4	)	(*n*=	7	)
V246R	-86.8	±	0.5	(κ=	8.0	±	0.4	)	(*n*=	6	)
L250R	-96.3	±	0.4	(κ=	6.8	±	0.3	)	(*n*=	6	)
I253R	-88.5	±	0.5	(κ=	7.1	±	0.5	)	(*n*=	6	)
L257R	-83.6	±	0.3	(κ=	6.0	±	0.3	)	(*n*=	6	)
K249E	-77.4	±	0.7	(κ=	9.1	±	0.7	)	(*n*=	6	)
E251K	-57.7	±	0.7	(κ=	8.9	±	0.6	)	(*n*=	4	)
E254K	-63.9	±	0.5	(κ=	6.4	±	0.4	)	(*n*=	4	)
E251/E254K	-65.1	±	0.4	(κ=	8.4	±	0.3	)	(*n*=	4	)
R243E	-81.4	±	0.6	(κ=	8.1	±	0.6	)	(*n*=	5	)
R243A	-85.3	±	0.5	(κ=	6.3	±	0.5	)	(*n*=	5	)
T239V	-89.6	±	0.3	(κ=	4.8	±	0.3	)	(*n*=	5	)
Y242F	-75.3	±	0.2	(κ=	4.8	±	0.2	)	(*n*=	7	)
Y242A	-94.8	±	0.3	(κ=	7.2	±	0.2	)	(*n*=	5	)
G221A	-79.7	±	0.4	(κ=	5.2	±	0.4	)	(*n*=	6	)
NavBacL WT[7]	-83.2	±	0.7	(κ=	5.8	±	0.6	)			
NavBacL ΔC246	-93.8	±	0.8	(κ=	6.0	±	0.7	)	(*n*=	6	)
NavSheP WT[7]	-116.0	±	0.9	(κ=	9.5	±	0.9	)			
NavSheP ΔC245	-113.7	±	1.3	(κ=	7.7	±	1.1	)	(*n*=	5	)

The value of $V_{1/2}$ for inactivation is the membrane potential of 50% steady-state inactivation. The unit of a slope factor (κ) for the inactivation is millivolts pre *e*-hold change. All results are presented as mean ± S.E.